

# ELECTRON DRIVEN ILC POSITRON SOURCE WITH A LOW GRADIENT CAPTURE LINAC

Masao Kuriki\*, Takaomi Kakita, Tohru Takahashi,  
Hiroshima University, Higashi-Hiroshima, Japan  
Kentaro Negishi, Iwate University, Morioka, Japan

Toshiyuki Okugi, Tsunehiko Omori, Masanori Satoh, Yuji Seimiya, Junji Urakawa, Koaru Yokoya,  
Accelerator Lab., KEK, Ibaraki, Japan  
S. Kashiwagi, Tohoku University, Sendai, Japan

## Abstract

ILC (International Linear Collider) is  $e^+e^-$  linear collider in the next high energy program promoted by ICFA. In ILC, an intense positron pulse in a multi-bunch format is generated with gamma ray from Undulator radiation. As a technical backup, the electron driven positron source has been studied. By employing a standing wave L-band accelerator for the capture linac, an enough amount of positron can be captured due to the large aperture, even with a limited accelerator gradient. However, the heavy beam loading up to 2 A perturbs the field gradient and profile along the longitudinal position. We present the capture performance of the ILC positron source including the heavy beam loading effect.

## INTRODUCTION

ILC (International Linear Collider) [1] is an  $e^+e^-$  linear collider with 500 GeV CME in the first phase and 1000 GeV in the second phase. This is only way to realize the  $e^+e^-$  collision beyond 350 GeV CME beyond the limitation of a storage ring collider and is an official future project promoted by ICFA. ILC realize the high luminosity as high as  $3.0 \times 10^{34} \text{ cm}^{-2} \text{ s}^{-1}$  with a limited average current, 50  $\mu\text{A}$ . This current is much less than that in a storage ring, but it is a technical challenge, especially for positron source, because it corresponds to 50 times of that in SLC [2]. In the current design [1], the positron is generated by Undulator radiation driven by more than 150 GeV energy electron beam. The high energy electron driver ( $>150$  GeV) is shared leading a possible long commissioning time for the positron source because it can be operated after the electron main linac is established. To avoid this limitation, an electron driven positron source has been studied.

In the electron driven positron source, the electron driver can be a dedicated several GeV linac. solving the problem related to the beam sharing. The biggest technical challenge on the electron driven positron source is the possible damage on the positron production target. In the undulator positron production,  $7.8 \times 10^{13}$  positrons are generated in 0.8 ms (macro pulse length). If we assume the same time structure for the electron driven positron source, any target can not survive with this heavy thermal heat load and a shock wave induced by the incident beam [3].

Omori et al. proposed a new  $e^-$ -driven scheme relaxing the target load [4] by extending the effective macro pulse length from 0.8 ms to 64 ms. In this scheme, positrons are accelerated by normal conducting accelerator and heavy beam loading is expected. Satoh et al. [5] proposed a beam loading compensation for the travelling wave linac by amplitude modulation. Urakawa [6] proposed a fast amplitude modulation method by combining two RF sources with a fast phase switching. Seimiya, Kuriki, et al. [7] showed that an enough positron,  $3.0 \times 10^{10}$  per bunch can be generated by assuming the beam loading compensation.

In this study, we propose the electron driven positron source for ILC based on the preceding studies [4, 7]. In this study, we assume RF power source off-the-shelf or developed by existing technology. Comparing to the preceding studies, the accelerator gradient is much lower. In addition, we re-evaluated the accelerator gradient and the beam loading compensation ability on the L-band standing wave accelerator which is used in the capture linac (the 1st accelerator section) after the target by newly developed a multi-cell cavity model. In the following sections, we explain the whole system, a new model for standing wave accelerator based on the multi-cell, and the simulation results.

## THE ELECTRON DRIVEN ILC POSITRON SOURCE

Figure 1 shows schematically the electron driven ILC positron source [7]. The positron is generated by impinging the 4.8 GeV electron beam on W-Re target. AMD (Adiabatic Matching Device) is attached at the downstream of the target to compensate the transverse momentum of the generated positron. This is composed from axially symmetric longitudinal magnetic field is peaked (5 T) at the entrance and decayed down to 0.5 T which is kept over the capture linac which is composed from 28 of L-band standing wave accelerator tubes. Chicane is placed after the capture linac to remove electrons and positrons with a large energy deviation. The booster accelerates the beam up to 5 GeV. It is composed from L-band and S-band traveling wave tubes. ECS (Energy Compressor System) is composed from 4 chicanes and 3 L-band RF structures. This is very important to obtain a good positron yield.

The positron is generated in 1  $\mu\text{s}$  macro-pulse containing 136 bunches with 6.15 ns bunch spacing. This pulse is

\* mkuriki@hiroshima-u.ac.jp

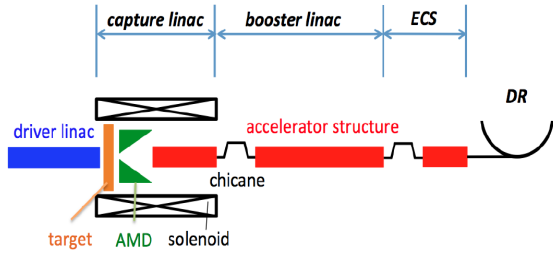


Figure 1: Schematic view of the electron driven ILC positron source. It consists from 4.8 GeV electron driver linac, target, AMD, capture linac, chicane, booster linac, and ECS.

repeated in 300 Hz for 64 ms of 200 ms. In the macro pulse, there are three intermediate gaps. In fact, this pattern is completely same as a part of the bunch fill pattern in DR (Damping Ring), where all bunches are stored for 136 ms to obtain the extremely small emittance beam. The positron bunches generated by the source are injected to DR with a long pulse kicker by keeping the pulse structure.

The electron driver employ S-band 3m normal conducting accelerators [8] by scaling the frequency to be 2.6 GHz. 80 MW klystron drives two accelerator tubes. By assuming 10% power loss in the wave guide, 36 MW RF input for each structure gives more than 40 MV/tube accelerator voltage. To obtain 4.8 GeV, we need 60 RF units.

The capture linac consists from L-band standing wave accelerators designed by J. Wang [9] originally for undulator positron source for ILC. 50MW L-band klystron drives two tubes. 14 units are assumed and the average energy after the capture section is 250 MeV.

After the capture linac, the positron is accelerated by the booster up to 5.0 GeV. The first half of the booster is composed from L-band accelerator to prevent the particle loss by the large aperture. We adopt 2m 1298MHz traveling wave accelerator designed for Super-KEKB [10] by scaling to 1.3 GHz. Two tubes are driven by one 50 MW klystron giving 21 MV/tube accelerator voltage with 0.78 A beam loading. The second half of the booster is composed from 2m S-band tubes for the better cost efficiency designed for Super-KEKB [11]. 80 MW klystron drives two tubes giving 31.5, MV/tube accelerator voltage. Total number of accelerator tubes are 116 L-band and 76 S-band for the booster.

The positron beam is then injected to DR (Damping Ring) through ECS (Energy Compressor System). The dynamic aperture of DR is given as [1].

$$\gamma A_x + \gamma A_y < 0.07 \quad (1)$$

$$\left(\frac{z}{0.035}\right)^2 + \left(\frac{\delta}{0.0075}\right)^2 < 1.0, \quad (2)$$

where  $A_x$  and  $A_y$  are the transverse action values,  $z$  and  $\delta$  are longitudinal position and the relative energy spread. Number of positrons in the DR acceptance normalized with the number of incident electron is defined as the positron yield. Our aim is to obtain an enough amount of positron in

the acceptance, that is  $3.0 \times 10^{10}$  positron / bunch including 50% margin.

## MULTI-CELL MODEL OF STANDING WAVE STRUCTURE

Here, we discuss performance of the standing wave accelerator used in the capture linac, because a large impact on the yield is expected. At the target, many electrons are also generated and contribute to the beam loading. As a result, a large beam loading is expected in the capture section before the chicane where electrons are removed.

The single cell model of a standing wave tube can be found in many places. The beam loading can be compensated with a appropriate conditions [12]. However, a real accelerator tube consists from multi-cells and each cells are connected through a finite coupling. As we will see later, the beam loading compensation is still effective, but the accelerator gradient is much less than that expected by the single cell model.

In the multi-cell model, voltage  $V_0$  of the coupling cell is expressed as [13]

$$\frac{dV_0}{dt} = - \left[ \frac{(1 + N\beta)\omega}{2Q} + k\omega \right] V_0 + \frac{1}{2}k\omega V_1 \quad (3)$$

$$+ \frac{1}{2}k\omega V_{-1} + \frac{\omega\beta}{Q} V_{in} - \frac{\omega RI}{2Q},$$

where  $V_1$  and  $V_{-1}$  are voltage of next cells,  $N$  is number of cells,  $V_{in}$  corresponds to input RF,  $Q$  is Q value of the cell and common for all cells,  $R$  is shunt impedance,  $k$  is coupling of cells,  $G$  is admittance, and  $I$  is the beam loading current. Similar expression can be made for all cells. Totally, we have N equations as

$$\frac{d\mathbf{V}}{dt} = \mathbf{A}\mathbf{V} + \mathbf{C}, \quad (4)$$

where  $\mathbf{V}$  is  $V_i$  vector,  $\mathbf{C}$  is a constant vector which contains beam loading terms, and  $\mathbf{A}$  is a real symmetric  $N \times N$  matrix.  $\mathbf{A}$  can be diagonalized with an orthogonal matrix  $\mathbf{R}$  as

$$\frac{d\mathbf{R}^T\mathbf{V}}{dt} = \mathbf{R}^T\mathbf{A}\mathbf{R}\mathbf{R}^T\mathbf{V} + \mathbf{R}^T\mathbf{C}. \quad (5)$$

By replacing a new base  $\mathbf{V}' = \mathbf{R}^T\mathbf{V}$ , the solution can be easily obtained. The cell voltage is expressed as a linear sum of the solution,

$$V_i(t) = \sum_{j=1}^N R_{ij} \tau_j C'_j (1 - e^{-\frac{t}{\tau_j}}). \quad (6)$$

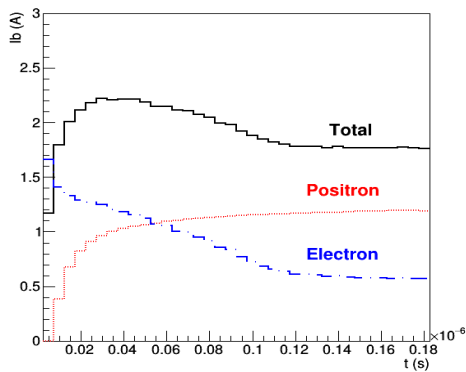
$\tau_i$  is the time constant of each modes,  $R_{ij}$  and  $C'_i$  are constants. The beam loading compensation was examined with this model and it was working well because few modes contribute to the acceleration. The fluctuation is less than 0.1% [13]. Table 1 shows a comparison of voltage by the single cell model and multi-cell model. There is a large discrepancy in the heavy load condition which might affect the positron yield.

Table 1: Accelerating Voltage by Two Models

Beam loading (A)	Single cell (MV)	Multi-cell (MV)
0 A	18.7	18.0
2.0 A	10.1	7.2

## SIMULATION

The simulation was performed in three steps. GEANT4 [14] was employed for the positron generation. 4.8 GeV electrons are impinged on 16mm thickness W-Re target and the generated particles are transferred to the next step. The beam size on the target was 3.5mm(RMS). From the downstream of the target to the capture section exit, GPT [15] performed the tracking. Figure 2 shows the beam loading current with the initial phase  $\phi = 2.0rad$ . The black solid line, red dotted line, and blue dashed line show the total current, positron, and electron contributions, respectively. Initially, the current by the positron and electron are cancelled each other, but it is rapidly increased up to 2.3 A by captured at different RF phase with  $\pi$  phase difference. In the simulation, the beam loading current is given as a function of longitudinal position (each tubes) prior to the simulation. This profile is tentatively determined by a pilot simulation and it was up to 2.0 A [13], which is smaller than the result in Fig. 2. The assumption in the simulation and the result should be even close to each other for consistency.

Figure 2: The beam loading current evolution for  $\phi = 2.0$ .

After the capture linac, chicane to remove electrons and positrons with a large energy deviation, a 5 GeV hybrid booster, ECS are simulated with SAD [16]. The conditions of the simulation is identical those in Ref. [7]. Figure 3 shows the positron yield as a function of the initial phase of the capture section. For each phase, booster RF phase are optimized for the maximum yield. Two peaks were observed in Fig. 3. The first peak at  $\phi = 2.0$  corresponds to deceleration capture condition where the positrons is placed on the deceleration phase initially in the capture linac. The positrons are finally captured at an acceleration phase by phase slip. The second peak at  $\phi = 4.0$  corresponds to acceleration capture. In this case, the positron is placed at the acceleration phase initially and captured at the same RF

phase. The yield is similar for these capture conditions, but the beam loading current is larger for acceleration phase, up to 4.0 A. From this reason, the deceleration phase is better solution.

By assuming 1.6 yield, the drive beam intensity is  $1.9 \times 10^{10}$  electrons/bunch which can be managed by the normal conducting S-band accelerator. The peak energy deposition density is expected to be 30 J/g which is below the practical limit developed by SLC operation, 35 J/g [17]. The beam loading current in the capture linac is, however, expected to be 2.2 A which is 10% larger than the assumption in the simulation. We have to iterate the simulation to obtain a consistent solution.

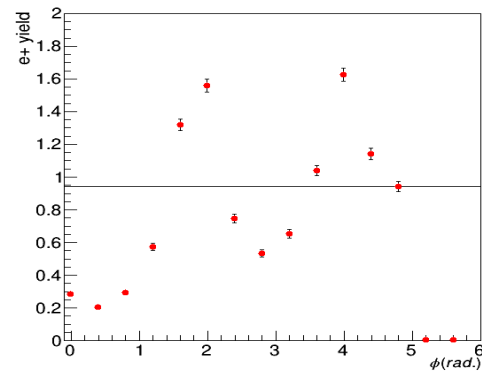


Figure 3: The positron yield as a function of the initial phase of the capture linac.

## SUMMARY

A start-to-end simulation for the electron driven ILC positron source was performed. By assuming conservative RF configurations and quantifying the accelerator voltage of the standing wave L-band accelerator with a multi-cell model, the accelerator field on the capture linac was decreased down to 5.6 MV/m. The simulation was done with GEANT4, GPT, and SAD and the positron yield was evaluated with DR acceptance to be up to 1.6. The expected peak energy deposition density on the target is below the practical limit. However, the beam loading current is 7% larger than the assumption to obtain the accelerator gradient and several iterations are needed to find a consistent solution.

## REFERENCES

- [1] ILC Technical Design Report (2013).
- [2] SLC Design Handbook, SLAC Report (1984).
- [3] M. Kuriki *et al.*, *PRSTAB* **9**, 071002(2006).
- [4] T. Omori *et al.*, *NIM A* (672) (2012)52.
- [5] M. Satoh *et al.*, *NIM A* 538 (2005) 116-126.
- [6] J. Urakawa, in *Proc. of Posipol 2014*, Ichinoseki, Japan (2014).
- [7] Y. Seimiya *et al.*, *PTEP* (2015) 103G01.
- [8] Hinode *et al.*, ATF design report.
- [9] J.W. Wang *et al.*, SLAC-PUB-12412 (2007).

- [10] S. Matsumoto *et al.*, "L-band Accelerator System in Injector Linac for SuperKEKB ", in *Proc. IPAC'10*, paper THPEA015 (2010).
- [11] S. Matsumoto *et al.*, "Large-aperture Travelling-wave Accelerator Structure for Positron Capture of SuperKEKB Injector Linac", in *Proc. IPAC'14*, paper THPRI047 (2014).
- [12] Handbook of Accelerator Physics and Engineering, World Scientific (1998).
- [13] M. Kuriki *et al.*, in *Proc. of PASJ*, paper WEOM06 (2016).
- [14] GEANT4, <https://geant4.web.cern.ch/geant4/>.
- [15] Pulsar Physics web site, [www.pulsar.nl/gpt/](http://www.pulsar.nl/gpt/).
- [16] SAD home page, [acc-physics.kek.jp/SAD/](http://acc-physics.kek.jp/SAD/).
- [17] S. Ecklund, SLAC-PUB-4437 (1987).